A high-performance low-cost constant-temperature hot-wire anemometer

1983 J. Phys. E: Sci. Instrum. 16 549

(http://iopscience.iop.org/0022-3735/16/6/022)

J. Phys. E: Sci. Instrum., Vol. 16, 1983. Printed in Great Britain

A high-performance low-cost constant-temperature hot-wire anemometer

E C Itsweire and K N Helland
Department of Applied Mechanics and Engineering Sciences and Institute for Pure and Applied Physical Sciences, University of California, San Diego, La Jolla, CA 92093, USA

Received 10 August 1981, in final form 25 October 1982

Abstract. A constant-temperature hot-wire anemometer circuit using a new, low noise and large frequency bandwidth operational amplifier is described. Dynamic tests showed that the circuit response was as fast as a commercial unit. Further measurements in various classical turbulent flows with hot wires and hot films, in air and water, proved the new circuit to have identical spectral behaviour and comparable noise levels with much simpler design and lower cost. In addition, the design of the circuit includes convenient features such as internal square-wave test, digital resistance dial for a wide range of overheat settings, and compensation for two cable lengths.

1. Introduction

Hot-wire anemometers operating at constant temperature have proved to be very useful instruments for measuring velocity fluctuations in turbulent flows. Complete reviews on constant-temperature anemometry have been presented by Kovasznay (1954), Corrsin (1963) and Comte-Bellot (1973, 1976) and numerous papers have analysed the feedback control theory associated with this anemometry (Freymuth 1967a, b, 1969, 1977b, Davis 1970, Perry and Morrison 1971).

The introduction of transistors and operational amplifiers made the design and construction of simple constant-temperature anemometers very easy (Kreider 1973, Miller 1976). Yet most references which suggest simple circuit designs do not include extensive comparisons with accepted high-quality commercial units. In particular they do not demonstrate their utility in special situations such as very small overheat or large velocity fluctuations. A small overheat, 5%, is necessary when one wants to measure turbulent velocity in mixtures such as air–helium, when contamination by large density fluctuations can be preponderant. In the case of large turbulent fluctuations the response of the anemometer circuit must be linear at every frequency. This work presents a circuit that uses a new high-performance operational amplifier which satisfies all the previous requirements, at a low cost. Since the circuit is of high order, a detailed feedback control theory analysis was not possible and was replaced by both dynamic tests and experimental comparisons with commercial units of high quality and reliability. Experiments covered two different fluids (air and water), two different kinds of velocity sensors (hot-wire and hot-films), and in some cases, two probe cable lengths (5 and 20 m).

Table 1. Characteristics of the OP-37 op amp.

Drift	$0.2\,\mu$V K^{-1} and $0.2\,\mu$V month^{-1}
Noise	$< 80\,\eta$V p–p 0.1 Hz to 10 Hz bandwidth
$1/f$ corner	2.7 Hz
Response	Slew rate: 17 V μs^{-1}
	Gain bandwidth: 63 MHz

2. Analysis of the circuit

The anemometer circuit has been designed at the University of California, San Diego. The main amplifier is a new ultra-low

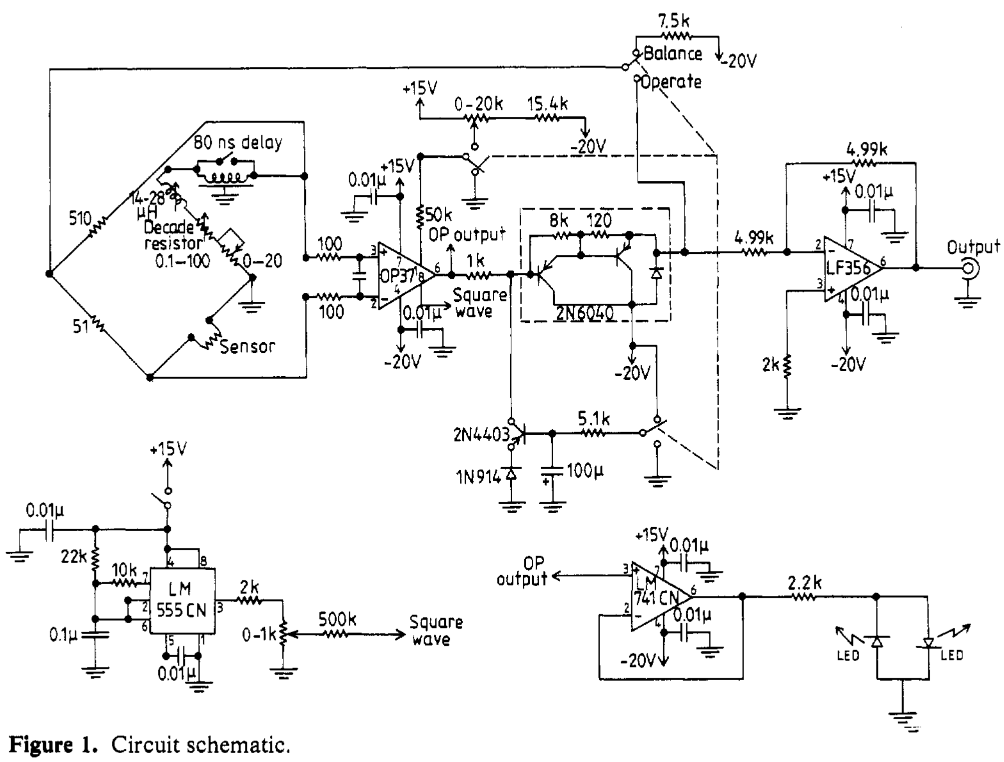

Figure 1. Circuit schematic.

noise, high-speed operational amplifier by Precision Monolithics Inc. Its main characteristics are given in table 1.

The schematic diagram of the circuit presented in figure 1 consists of a fairly classical feedback loop system using two amplification stages. The bridge used has a 10:1 ratio which makes it convenient to use a dialable decade resistor for measuring the sensor resistance and setting the overheat. As further results will show, this relatively high ratio does not impede anemometer performance.

The output signal of the bridge is fed to the low-noise OP-37 operational amplifier and then to a Darlington amplification stage before being fed back to the bridge. It is very critical to the performance of the circuit that the feedback signal be in phase with the original sensor signal. Therefore in order to compensate for the sensor cable resistance, inductance and capacitance, the bridge includes a small adjustable resistor and a delay line. We chose to compensate for 5 and 20 m cable lengths for which most of our laboratory experiments are performed. Probably, longer cables such as 50 or 100 m could be compensated in a similar fashion. For the 5 m cable a variable inductor was used, neglecting capacitance effects, whereas an 80 ns delay line simulating the cable was added for the 20 m cable. A buffer amplifier was placed after the Darlington stage output to decouple the circuit from the output connector.

The square-wave generator primarily consists of a 300 Hz integrated oscillator with adjustable test signal amplitude as shown in the lower left corner of figure 1. The balance indicator system, shown in the lower right corner, uses the OP-37 as a comparator. The balance circuit is sensitive to the smallest change allowed by the decade resistor.

The circuit has been built in a Tektronix module as shown in figure 2. This module is compatible with the Tektronix TM 500 main power frame. The printed circuit board has a ground plane to reduce noise to a minimum and the circuit parts are shielded to minimise 60 Hz pick-up from the power supply. The parts cost of one unit as shown in figure 1 is about US $200.

Figure 2. Front panel of UCSD constant-temperature anemometer.

3. Response to square-wave test

Both the commercial and the UCSD anemometer have a built-in signal generator used to feed a square-wave test signal into the circuit. The transient response to both rising and falling edge of the square wave was observed on an oscilloscope connected to the output of the anemometer. In the UCSD circuit the square wave is introduced as an offset of the OP-37. The measurements shown in table 2 were made for a critically damped or slightly underdamped response under several experimental conditions. Figure 3 shows the time reponse to a square wave for such damping conditions. For the hot-film sensors we estimated the time constant τ using the technique of Freymuth and Fingerson (1977). Freymuth (1977a) gives a relation to approximate the cut-off frequency of the circuit in that case as: $f_{\text{cutoff}} = 1/1.5\,\tau$. Results compared to typical highest frequencies present in turbulent flows are shown in table 3. All the estimated cut-off frequencies are inside the range of experimental conditions.

4. Side-by-side comparison in several turbulent flows

After satisfactory results were obtained for both square-wave tests and peak-to-peak noise measurements observed on an oscilloscope, we performed a side-by-side comparison of our circuit with recent commerical units of accepted quality under conditions covering a wide range of experiments, in air using hot-wire and hot-film sensors, and in water using a quartz-coated film.

The general experimental set-up is the same for all experiments and is shown in figure 4. In order to eliminate as much noise as possible, the data were digitised directly and stored on digital tape before analysis. Calibration and data computations were performed shortly after each experiment. Most of the measurements were performed using a standard 5 m cable between probe support and anemometer and some using a 20 m cable.

Table 2. Square-wave test results.

Experiment	No.	Speed U(m s^{-1})	Sensor	Overheat	Time response $\tau(\mu s)$ DISA	UCSD
Biplane grid	1	10.6	Hot wire	50%	15	15
Biplane grid	2	10.6	Hot wire	5%	50	40
Air jet	3	7.9	Hot wire	50%	20	15
Biplane grid	4	10.6	Air film	50%	50	40
Water jet	5	0.46	Water film	10 K	40	40

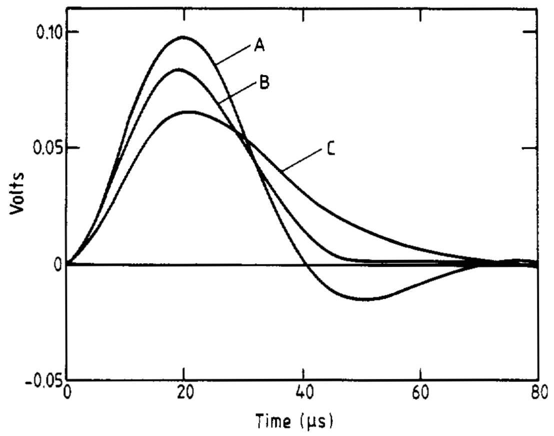

Figure 3. Square-wave responses: A, under-damped; B, critically damped; C, over-damped.

4.1. Nearly isotropic grid-generated wind tunnel turbulence

Three different sets of measurements were taken using a single hot-wire probe TSI T20 with a platinum-plated rhodium wire having a sensing length of $l=1$ mm and a diameter $d=5$ μm. The sensor was located downstream of a biplane grid of mesh size $M=25.4$ mm (1 in) at a distance $x/m=36$ in the low-speed low-turbulence wind tunnel of the Department of Applied Mechanics and Engineering Sciences at the University of California, San Diego. First, measurements were taken at a mean speed $U=10.6$ m s^{-1} with a turbulence intensity $u'/U=1.6\%$. A set of measurements were made using commercial units from a DISA 55M01 and a TSI 1054 at an overheat of 0.5 in order to check if their response was the same. The results showed excellent agreement, as expected, for the power spectrum $E_{uu}(f)$ over a 10 kHz bandwidth. This result has been verified for the higher frequencies by looking at $f^2E_{uu}(f)$. Next, measurements were taken both with our circuit and the DISA at two overheats, 0.5 and 0.05 respectively, under the operating conditions described above. Both comparisons (curves A and B in figures 5 and 6) show excellent agreement

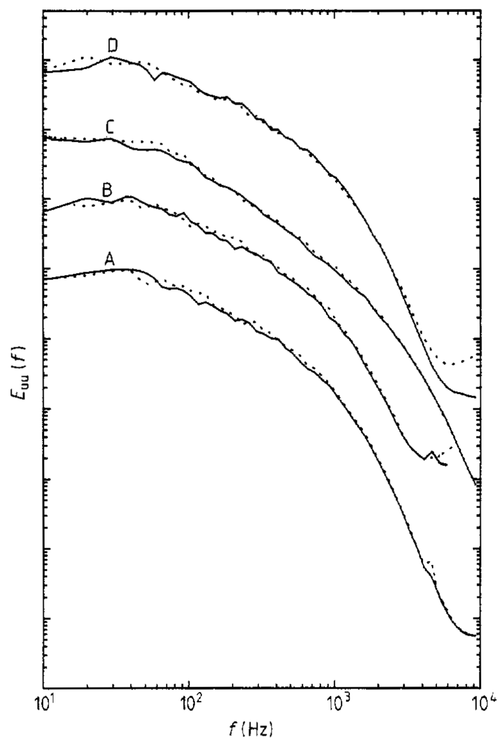

Figure 5. Velocity power spectra: ——, DISA; - - -, UCSD; A, grid turbulence, hot-wire, overheat 50%; B, grid turbulence, hot-wire, overheat 5% (shifted up one decade); C, turbulent jet, hot-wire, overheat 50%; D, grid turbulence, hot-film, overheat 50% (shifted up three decades).

even for the high frequencies; the signal-to-noise ratio is also comparable. The same measurement was successfully repeated using a 20 m cable at a 0.5 overheat.

4.2. Axisymmetric air jet

This test was performed in order to verify that the frequency response of the anemometer circuit was linear, i.e., independent

Table 3. UCSD anemometer frequency response.

Experiment	Time response $\tau(\mu s)$	Cut-off frequency f_{cut}(kHz)	Typical max. frequency f_{max}(kHz)
1	15	44.4	10
2	40	16.7	10
3	15	44.4	15
4	40	16.7	10
5	50	13.3	0.4

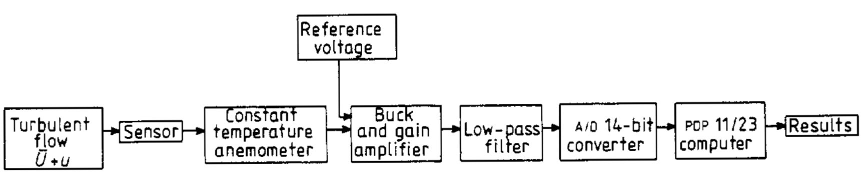

Figure 4. Experimental set-up

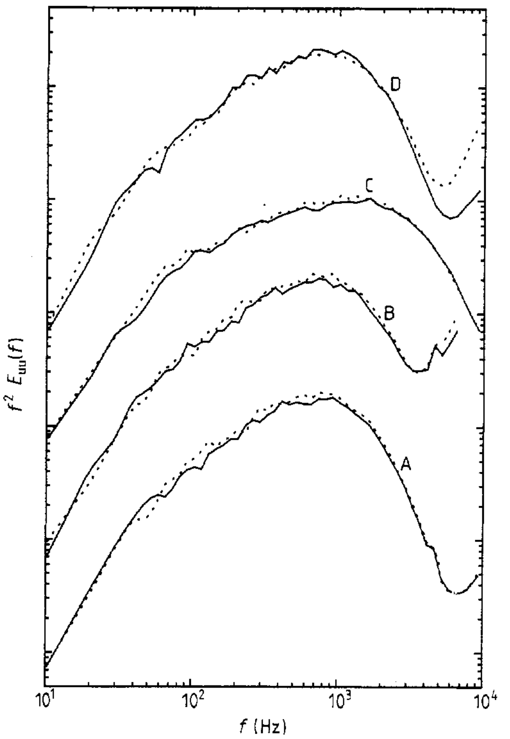

Figure 6. Velocity derivative power spectra: ——, DISA; - - -, UCSD; A, grid turbulence, hot-wire, overheat 50%; B, grid turbulence, hot-wire, overheat 50% (shift up one decade); C, turbulent jet, hot-wire, overheat 50%; D grid turbulence, hot-film, overheat 50% (shifted up three decades).

of the amplitude of the fluctuations. The turbulence intensity on the centreline of the jet at $X/D = 10$ was $u'/U = 25\%$ and the mean speed $U = 7.9$ m s^{-1} corresponding to a jet velocity $U_{jet} = 12$ m s^{-1}. The power spectra (figure 5, C) show excellent spectral behaviour for the air circuit in the inertial range (−5/3) law) and the viscous range (−4 law), which is verified by the collapse of the $f^2E_{uu}(f)$ curve C in figure 6.

4.3. *Air film measurements*

Measurements using a hot film for use in air were performed under experimental conditions described in § 4.1. The sensor was a TSI cylindrical film Model 1210-20 with an overheat of 0.5. Again the spectral behaviour of both circuits show good agreement (D, figures 5 and 6). As in the case of the other hot-film test, the noise level for the UCSD anemometer is slightly higher (+3 dB) than for the DISA. Perhaps some of the noise can be attributed to the prototype circuit board used for the test experiments which did not have a ground plane and optimum component layout.

4.4. *Axisymmetric water jet*

The anemometer test was repeated for a water jet using a hot-film sensor to check the reponse of the anemometer circuit when connected to another type of sensor. A hot film, due to different geometrical and physical properties, responds differently from a hot wire. Also the highest frequencies observed in water are only several hundred Hertz compared to several thousand Hertz in air.

The jet velocity was $U_{jet} = 1.5$ m s^{-1} and the film was located in the centreline of the jet at $X/D = 20$. The film mounted on a TSI T20 support was a cylindrical quartz-coated 1210-20 film for use in salt water.

Results presented in figure 7 show good agreement between both anemometers. This is remarkable since the DISA unit has an external switch for films in order to correct the frequency response of their circuit. Limitations of the power supply voltage to +20 V by the OP-37 excluded the use of high overheat when using sensors of impedance larger than about 10 Ω.

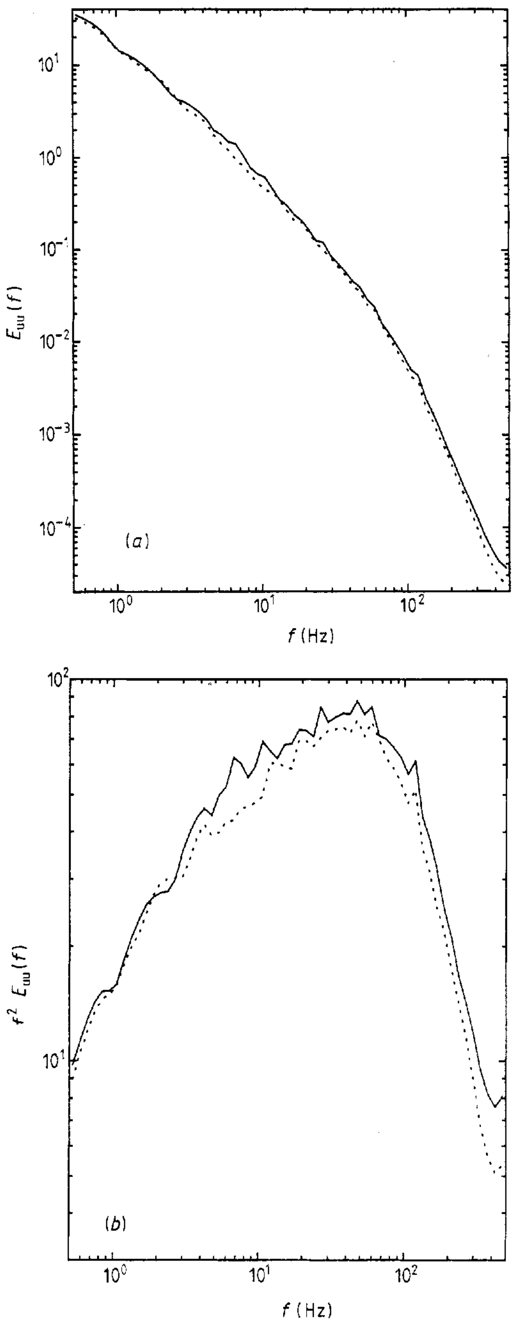

Figure 7. (*a*), Velocity power spectra of water jet. (*b*), Derivative power spectra of water jet. ——, DISA; - - -, UCSD.

5. Conclusions

Perry and Morrison (1971) showed that the bridge inductance is the dominant factor in obtaining good frequency response and not the amplifier response. We have incorporated this design consideration in the present constant-temperature anemometer circuit.

While avoiding too much complexity, our design achieves results of comparable quality to two commercial units. Our aim was to produce a low-cost unit for multi-sensor turbulent measurements under various experimental conditions and also having all the convenient additional features and performances of commercial units. This goal was successfully achieved as demonstrated in all the spectral comparisons.

Acknowledgments
The authors wish to express their appreciation to Jon Haugdahl and Michael Head for their help in designing and testing of the circuit. Financial support from NSF grants OCE78-09060 and MEA81-00431 is gratefully acknowledged.

References

Comte-Bellot G 1973 Anémometrie à fil chaud *CEA-EDF Cycle de conférences sur les techniques de mesure dans les écoutements*. E4, 1–82

Comte-Bellot G 1976 Hot-wire anemometry *Ann. Rev. Fluid Mech.* **8** 209

Corrsin S 1963 Turbulence: experimental methods *Handbuch der Physik* (Berlin: Springer) Vol. VIII, 2, pp 524–90

Davis M R 1970 The dynamic response of constant resistance anemometers *J. Phys. E: Sci. Instrum.* **3** 15–20

Freymuth P 1967a Feedback control theory for constant-temperature hot-wire anemometers *Rev. Sci. Instrum.* **38** 677–81

Freymuth P 1967b Noise in hot-wire anemometers *Rev. Sci. Instrum.* **39** 550–7

Freymuth P 1969 Nonlinear control theory for constant-temperature hot-wire anemometers *Rev. Sci. Instrum.* **40** 258–62

Freymuth P 1977a Frequency response and electronic testing for constant-temperature hot-wire anemometers *J. Phys. E: Sci. Instrum.* **10** 705–10

Freymuth P 1977b Further investigation of the non-linear theory for constant-temperature hot-wire anemometers *J. Phys. E: Sci. Instrum.* **10** 710–3

Freymuth P and Fingerson L M 1977 Electronic testing of frequency response for thermal anemometers *Thermo-Systems, Inc., Quarterly* 3, Nov–Dec 5, 12

Kovasznay L S G 1954 Turbulence measurements *Physical measurements in gas dynamics and combustion* (Princeton, New Jersey: Princeton University Press) Section F, 2, pp 219–76

Kreider J F 1973 A simple, stable constant-temperature hot-wire anemometer *IEEE Trans. Instrum. Meas.* **IM-22** 190–1

Miller J A 1976 A simple linearized hot-wire anemometer *J. Fluid Engng* **98** 749–52

Perry A E and Morrison G L 1971 A study of the constant-temperature hot-wire anemometer *J. Fluid Mech.* **47** 377–599